Conformational Change of Poly(*N*-isopropylacrylamide) during the Coil−Globule Transition Investigated by Attenuated Total Reflection/Infrared Spectroscopy and Density Functional Theory Calculation†

Yukiteru Katsumoto,‡ Takeyuki Tanaka,‡,§ Harumi Sato,‡ and Yukihiro Ozaki*,‡

Department of Chemistry, School of Science, Kwansei-Gakuin University, 2-1 Gakuen, Sanda, Hyogo 669-1337, Japan, and Graduate School of Science and Technology, Kobe University, Rokkodai, Nada-ku, Kobe 657-8501, Japan.

Received: July 2, 2001; In Final Form: September 27, 2001

A conformational change in the coil−globule transition of poly(*N*-isopropylacrylamide) (PNiPA) was investigated by Fourier transform infrared (FT-IR) spectroscopy with attenuated total reflection (ATR) method and density functional theory (DFT) calculations. ATR/IR spectra of PNiPA in an aqueous solution change dramatically in the vicinity of the coil−globule transition temperature (θ temperature). Below the θ temperature, unimodal peaks are observed at 1624 cm^{-1} in the amide I region and at 1562 cm^{-1} in the amide II region, respectively. Above the θ temperature, a new peak appears abruptly near 1653 cm^{-1} in the amide I region and the amide II band shifts gradually to a lower frequency by 6 cm^{-1}. In the amide III region, the relative intensity of a band at 1173 cm^{-1} is weaker than that of a band at 1155 cm^{-1} at lower temperatures, but it becomes larger during the coil−globule transition of PNiPA. DFT calculation for dimer models of PNiPA suggests that the amide I band at 1624 cm^{-1} is assigned mainly to a stretching vibration of the C═O group that forms a strong hydrogen bond with the N−H bond of a neighboring amide group. The band at 1653 cm^{-1} observed above the θ temperature may be due to a free C═O group. It is, therefore, suggested that some of the intramolecular hydrogen bonds between neighboring amide groups are broken during the coil−globule transition. Furthermore, it is deduced from the DFT calculation that the relative intensity of the bands at 1173 and 1155 cm^{-1} in the amide III region reflects the population change in the gauche and trans conformations in the main chain during the coil−globule transition.

Introduction

Conformational changes of polymers have attracted many scientists because microscopic structures of polymers are reflected on macroscopic properties of those systems.[1] In general, the factors that cause conformational changes of a polymer are categorized into two kinds of interactions: the short-range interaction and the long-range interaction.[2,3] The short-range interaction is due to the interaction within a few neighboring segments along the main chain. On the other hand, segments distant along the main chain do interact if they come close to each other in space. Such an interaction is often called the long-range interaction in contrast to the short-range interaction. These interactions arise from van der Waals interaction, chemical bonds between side chains (e.g., hydrogen bonding and disulfide bonding), affinity between polymers and solvents (e.g., hydrophobic interaction), electrostatic interactions (e.g., electric dipoles and electrolytes), topological interactions (e.g., entanglements), and so on. It is considered that the coil−globule transition of a polymer is caused by these interactive forces.[4−6]

As one of the fundamental problems in polymer physics, the coil−globule transition has been widely studied in the last three decades[4−11] because it is concerned with many aspects of the polymer dynamics such as phase separations of a polymer solution, morphological formations of a biopolymer, and collapses of a polymer gel. The coil−globule transition of poly(*N*-isopropylacrylamide) (PNiPA) has received particularly keen interest because it is a nonionic polymer that has the coil−globule transition temperature called θ temperature[2] near room temperature in an aqueous solution.[12,13] One of the most curious points in the studies of PNiPA lies in the characteristic property of its hydrogels. The hydrogels of PNiPA are well-known to show a volume phase transition in response to temperature change; that is, the gels discontinuously collapse above the transition temperature.[14] A theoretical approach based on the Flory−Huggins theory suggests that a discontinuous volume change of a gel occurs when an external stress is imposed upon it.[15] That is to say, the phase transition of the gels is considered as a macroscopic manifestation of the coil−globule transition of polymers. This may be the reason the studies on the coil−globule transition of PNiPA attract many scientists.

The PNiPA chain is in an extended coil state below the θ temperature (ca. 32 °C) and collapses to a globule state above the θ temperature. The transition behavior of PNiPA has been explored extensively by use of various experimental techniques, e.g., turbidity,[12,16] light scattering,[17,18] calorimetry,[19,20] fluorescence,[21,22] nuclear magnetic resonance,[23] and IR spectroscopy.[24−26] In general, the coil−globule transition of PNiPA has been explained by the following mechanism.[4,12,13,16−26] Below the θ temperature, the polymer assumes an extended coil conformation because the segment−solvent contacts are favored. On the other hand, the attractive interaction among the segments induces the coiled polymer chains to collapse into a globular state. There have been many reports that have attempted to elucidate the long-range interaction of polymers on the basis of changes in

† Part of the special issue "Mitsuo Tasumi Festschrift".

* To whom correspondence should be addressed. Fax: +81−795−65−9077. E-mail: ozaki@kwansei.ac.jp.

‡ Kwansei-Gakuin University.

§ Kobe University.

10.1021/jp0124903 CCC: $22.00
Published on Web 12/14/2001

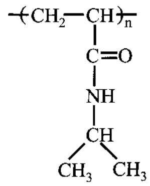

Figure 1. Chemical structure of PNiPA.

an affinity between polymer segments and solvents.[17−26] However, PNiPA has amide groups as its side chains. It is well-known that amide groups can form a strong hydrogen bond in an aqueous solution. For example, the hydrogen bond among the amide groups causes the helix−coil transition of polypeptides.[27,28] However, the influences of the hydrogen bonds among the amide groups on the coil−globule transition of PNiPA have not been well investigated. To understand more deeply the mechanism of coil−globule transition of PNiPA, it is desirable to investigate the changes in the hydrogen between the amide groups during the coil−globule transition of PNiPA.

The purpose of the present study is to investigate the hydrogen bonds of amide groups and the conformation of the main chains of PNiPA by use of IR spectroscopy and density functional theory (DFT) calculation with the aim of elucidating the short-range interaction of PNiPA. IR spectroscopy is one of the most useful techniques for investigating changes in the microscopic environment around amide groups and conformational changes in polymer main chains.[29] Although there were some reports on the coil−globule transition of PNiPA studied by IR spectroscopy,[23−25] the spectral changes have not fully been analyzed; the band assignments of PNiPA are still ambiguous even in the amide I and II regions, and bands that are due to the backbones have never been discussed. This study provides new insight into thermal changes in the IR spectra of PNiPA by using the spectral analysis method and DFT calculation.

Experimental Section

Sample Preparation. *N*-isopropylacrylamide (Tokyo Kasei Kogyo Co. Ltd., Tokyo, Japan) was purified by recrystallization from a benzene/*n*-hexane (1:6) mixture solution. PNiPA was synthesized by radical polymerization in benzene using 2,2′-azobis(isobutylonitrile) as an initiator. The reaction was carried out for 1 h at 60 °C under nitrogen. The details of polymerization are described elsewhere.[30] The polymer synthesized was purified by reprecipitation from *n*-hexane, and the precipitate was dried under vacuum for 24 h. Figure 1 shows the chemical structure of PNiPA. PNiPA dissolved in distilled water (20 g/L) was incubated at ca. 10 °C for 12 h before IR measurements. A cast film of PNiPA was prepared by putting one drop of an acetone solution of PNiPA on a CaF_2 plate. The film was dried in a vacuum for 12 h.

FTIR Measurement. The transmission and attenuated total reflection infrared (ATR/IR) spectra were measured at a 4 cm^{-1} resolution using a Nicolet Magna 760 Fourier transform IR spectrometer with a liquid-nitrogen-cooled mercury−cadmium−telluride detector. A total of 512 scans were co-added for each spectrum. An ATR cell was made of a horizontal ZnSe crystal (the refractive index is 2.403) with an incidence angle of 45° (Thermal A.R.K, Spectra-Tech, Inc.). The temperature of the ATR cell was controlled by a thermoelectric device (CN4400, OMEGA) with an accuracy of ±0.1 °C. The temperature was increased at a rate of ca. 2 °C/h. The temperature of the ATR cell was stabilized at 23.8 °C for 30 min before the measurements. After changing the temperature, the cell was maintained for 15 min to make the sample solution equilibrate at that temperature. The refractive index was measured by using an Abbe refractometer (NAR-1, ATAGO).

Data processing such as the subtraction of a water spectrum and the calculation of a second derivative spectra was performed by a program written in C++ language (Visual C++ 6.0, Microsoft). The second derivatives were calculated using the Savitzky−Golay method[31] with the number of smoothing points being equal to 7.

DFT Calculations. All DFT calculations were performed using a B3LYP functional.[32] In the DFT calculations, the structures of dimer models of PNiPA were optimized using the basis set of 6-31G(d), and the vibrational frequencies and intensities[33] were computed using basis sets of 6-31G(d), 6-31G-(d,p), 6-31+G(d), 6-31+G(d,p), and 6-31++G(d,p).[34−40] The computations were carried out with the Gaussian 98 program[41] at the Information Processing Center of Kobe University. The force fields calculated at the B3LYP/6-31G(d) level were scaled down using a single scale factor, 0.9613, which is accepted to be best for the level.[42] The scale factor was also multiplied into vibrational frequencies for the other basis sets. In order intuitively to compare the calculated frequencies and intensities with the observed ones, IR spectra of dimer models of PNiPA were simulated from the IR frequencies and intensities obtained at the DFT calculations, assuming that the band shapes and bandwidth were Lorentzian and 7 cm^{-1}, respectively. The vibrational assignments of the dimer models for PNiPA were carried out from the view of Cartesian normal coordinates by DFT calculation. In addition, DFT calculations on the basis of the Onsager reaction field model[43,44] were performed to investigate effects of hydration of PNiPA on the IR spectra into water because the model is the simplest one among various reaction field models and the calculation can converge in less computation time. The dielectric constant of a solvent and the radius of a spherical cavity are needed for the Onsager model. In the DFT calculation, the dielectric constant of water included in the Gaussian 98 program and the radius recommended by a single-point energy calculation at the B3LYP/6-31G(d) level were used for the Onsager model.

Results

1. Pretreatment Procedure for the ATR/IR Spectra of PNiPA. Figure 2a shows ATR/IR spectra of a PNiPA aqueous solution and water measured at 33.8 °C. IR spectra obtained by the ATR method are generally corrected to eliminate the dependence of the penetration depth.[45] The corrected spectra of the PNiPA aqueous solution and water are shown in Figure 2b. As seen in Figure 2b, the ATR/IR spectrum of the PNiPA aqueous solution is close to that of water. To distinguish characteristic bands of PNiPA, the spectrum of water, $I_w(\nu)$, was subtracted from the spectrum of the PNiPA aqueous solution, $I_s(\nu)$, as follows. The region between 1750 and 2700 cm^{-1} is essentially devoid of PNiPA bands. Therefore, referring to this region, the quantitative subtraction of the water spectrum is possible.[46,47] A subtracted spectrum $I_{sub}(\nu)$ is calculated by the following equation:

$$I_{sub}(\nu) = I_s(\nu) - \alpha I_w(\nu) + \beta \tag{1}$$

where α and β are scaling and correction factors for the baseline shift, respectively. For the quantitative subtraction, α and β can be determined by using the following conditions:

$$\sum_i (I_s(\nu) - \alpha I_w(\nu) + \beta)^2 = \text{minimize}, \qquad \nu_{min} \le \nu \le \nu_{max} \tag{2}$$

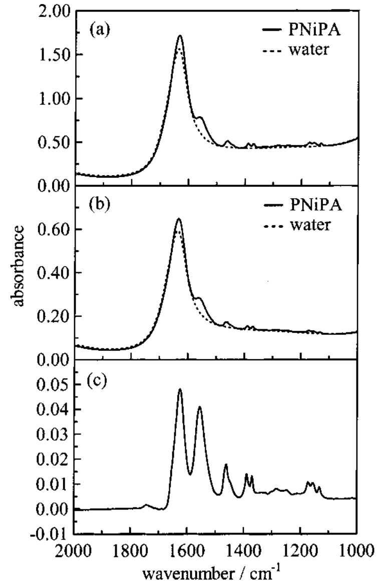

Figure 2. (a) ATR/IR spectra in the 2000−1000 cm^{-1} region of water and the aqueous solution of PNiPA at 33.1 °C. (b) ATR/IR spectra of water and the PNiPA aqueous solution after the correction for the dependence of the penetration depth. (c) A difference spectrum obtained after the subtraction of the spectrum of water from that of the PNiPA aqueous solution.

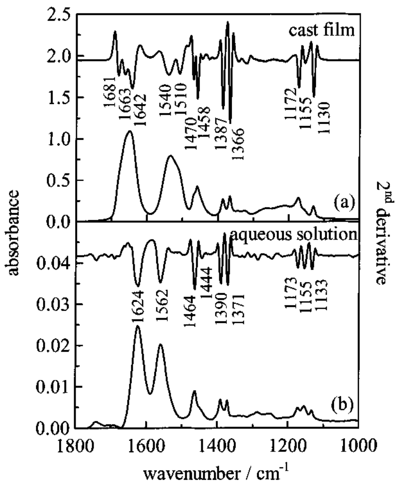

Figure 3. (a) IR spectrum of a PNiPA cast film and its second derivative. (b) ATR/IR spectrum of a PNiPA aqueous solution at room temperature (ca. 24 °C) and its second derivative.

This method proposed in the present study for the subtraction of the water spectrum has provided better results, at least, for the ATI/IR spectra of PNiPA aqueous solutions than for the previously proposed methods.[46,47] Figure 2c shows the subtracted spectrum for PNiPA, in this case, using the range of $\nu_{\min} =$ 1760 and $\nu_{\max} = 2000$ with the value of $\alpha = 0.9535$ and $\beta =$ 0.00246. As can be seen in Figure 2, parts b and c, the absorbance of PNiPA is approximately 10 times smaller than that of water in the amide I (near 1620 cm^{-1}) region. Thus, a careful treatment is necessary to obtain reliable difference spectra.

2. Comparison of IR Spectra of a Cast Film and an Aqueous Solution of PNiPA. Figure 3 represents IR spectra of a cast film and an aqueous solution of PNiPA at room temperature (ca. 24 °C) together with their second derivative spectra. Prominent IR bands are amide I, II, and III bands; deformation bands due to the isopropyl group; and C−H bending vibration bands. The wavenumbers and assignments of the observed bands are summarized in Table 1. The vibrational assignments written in Table 1 were ascertained from the view of Cartesian normal coordinates by DFT calculations described later.

TABLE 1: Vibrational Assignments for the Relevant Peaks in the Observed IR Spectra of the Aqueous Solution and the Cast Film of PNiPA

wavenumber/cm^{-1}		
aqueous solution	cast film	assignment
1650[a]	1681	amide I
1624	1663	amide I (hydrogen bonding)
	1642	amide I
1562	1540	amide II (hydrogen bonding)
	1510	amide II
1464	1470	CH_3 asym. deformation[b]
1444	1458	CH_3 asym. deformation[b]
1390	1387	CH_3 sym. deformation[b]
1371	1366	CH_3 sym. deformation[b]
1173	1172	amide III
1155	1155	amide III
1133	1130	CH_3 rock[b]

[a] Observed above the θ temperature. [b] Vibrational mode associated with the methyl group of the isopropyl group.

Remarkable differences between these two spectra are observed in the regions of amide I and amide II bands. The spectrum of the cast film shows, at least, three and two component bands in the amide I and amide II regions, respectively. The calculation of the second derivative confirms this. In the spectrum of the aqueous solution, the amide I band shifts largely to a lower frequency, whereas the amide II band shows a distinct high-frequency shift. Both amide I and II bands become sharp, and the second derivative spectrum suggests that each band consists of only one component band. An amide I band contains the contribution mainly from a C═O stretching vibration, and an amide II band is due to the coupling of a N−H bending and C−N stretching vibrations. The C═O group of an amide group of PNiPA can form hydrogen bonds with the N−H group of a neighboring amide group and/or with water. Thus, the frequencies of amide I and amide II bands reflect the strength of the hydrogen bond and the electron density on C═O and N−H bonds. When the C═O bond of PNiPA forms a hydrogen bond, the amide I band shifts to a lower frequency compared with the frequency of amide I band because of the "free" C═O group. On the other hand, a hydrogen bond of the N−H group causes an upward shift of the amide II band. The observations shown in Figure 3 suggest that the C═O and N−H groups of the PNiPA side chains form the hydrogen bonds and/or are hydrated in the aqueous solution. It goes without saying that a change in the permittivity around the polymer has an effect the band shifts.

The relative intensity of a band at 1155 cm^{-1} of the cast film is also different from that of the aqueous solution. Although the band at 1155 cm^{-1} appears as a shoulder of the band at 1173 cm^{-1} in the spectrum of the cast film, it becomes an isolated peak in the spectrum of the aqueous solution. The distinct variation of the band at 1155 cm^{-1} suggests that the band is sensitive to changes of polymer conformations and/or the local environment around the polymer segments. This will be discussed later in more detail.

3. Temperature-Dependent Changes in IR Spectra of a PNiPA Aqueous Solution. Figure 4 depicts difference ATR/IR spectra of PNiPA in an aqueous solution measured over a temperature range of 23.7−38.2 °C at an increment of ca. 0.8

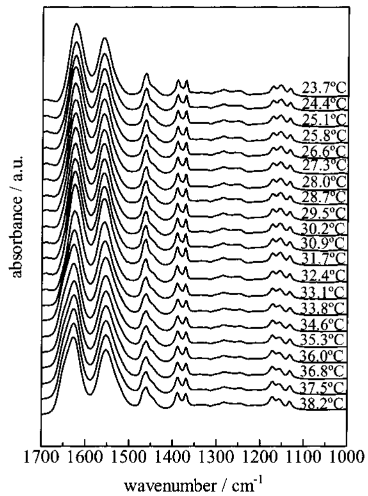

Figure 4. Temperature-dependent changes in ATR/IR spectra of PNiPA in an aqueous solution. Temperature was varied from 23.7 to 38.2 °C at increments of ca. 0.8 °C.

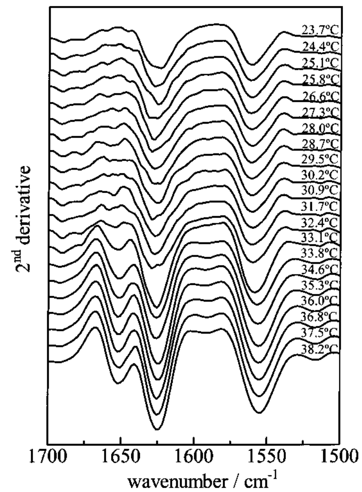

Figure 5. Second derivatives in the 1700−1500 cm^{-1} region of the spectra shown in Figure 4.

°C. In this section, temperature dependent changes of the spectra are investigated in detail by using several spectral analysis methods.

In the vicinity of the θ temperature (ca. 32 °C), a coiled conformation of PNiPA chain collapses and becomes a globular conformation.[12,13,16−26] Above the transition temperature, the globular chains of PNiPA aggregate each other and precipitate. Therefore, the intensities of IR bands of PNiPA are expected to change abruptly near the θ temperature. For the overview of these intensity variations, the calculation of a derivative for the intensity profile is useful. Let us consider an observed IR absorbance intensity $I(\nu,T)$ as functions of frequency ν and temperature T. A partial differentiation for T can be calculated as $\partial I(\nu,T)/\partial T$. As can be seen in Figure 4, structural changes of PNiPA may cause not only a change in the absorbance intensity but also a variation in the band shape. For example, changes in bandwidth (broadening or narrowing) and peak position may be observed during the transition. For a target band that has a peak at a frequency ν_0 observed at T_i, the cross correlation coefficient $R_{\nu_0}(T_i,T_j)$ is calculated with a spectral area using eq 3, where the obtained spectra are numbered in order of T by suffix i (i = 0,1,2, ...):

$$R_{\nu_0}(T_i,T_j) = \frac{\sum_{k=-m}^{m} \{I(\nu_k,T_i) - \overline{I(\nu_0,T_i)}\}\{I(\nu_k,T_j) - \overline{I(\nu_0,T_j)}\}}{[\sum_{k=-m}^{m} \{I(\nu_k,T_i) - \overline{I(\nu_0,T_i)}\}^2 \sum_{k=-m}^{m} \{I(\nu_k,T_j) - \overline{I(\nu_0,T_j)}\}^2]^{1/2}} \quad (3)$$

where

$$\overline{I(\nu_0,T_i)} = \frac{1}{2m+1} \sum_{k=-m}^{m} I(\nu_k,T_i) \quad (4)$$

Notice that ν_{-m} and ν_m define the lower and upper limits for the calculation range. The above cross correlation coefficient has been introduced in the present study to probe a change in a band shape clearly. For the spectra observed here, the calculation range of ca. ±20 cm^{-1} is adopted. A cross correlation coefficient calculated from eq 3 is an index of the linear combination between $I(\nu_0,T_i)$ and $I(\nu_0,T_j)$. $R_{\nu_0}(T_i,T_j)$ becomes equal to 1 when the linear combination is kept between $I(\nu_0,T_i)$ and $I(\nu_0,T_j)$. An $R_{\nu_0}(T_i,T_j)$ value smaller than 1 indicates that the band shape near ν_0 varies with the change of temperature from T_i to T_j. Thus, the $R_{\nu_0}(T_i, T_j)$ value is quite sensitive to the change of a band shape near a frequency ν_0, whereas it is insensitive to the intensity variation. That is, the variations of a band shape near a target band can be discussed only with reference to the $R_{\nu_0}(T_i,T_j)$ value.

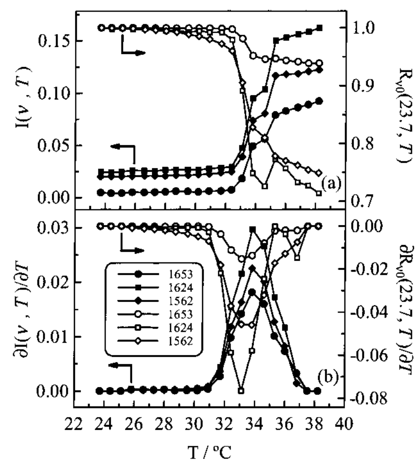

Figure 6. (a) $R_{\nu_0}(23.7,T)$ for the bands at 1653 cm^{-1} (the opened circle), 1624 cm^{-1} (the opened square), and 1562 cm^{-1} (the opened diamond). $I(\nu, T)$ for the bands at 1653 cm^{-1} (the closed circle), 1624 cm^{-1} (the closed square), and 1562 cm^{-1} (the closed diamond). (b) First derivatives of $R_{\nu_0}(23.7,T)$ and $I(\nu,T)$ displayed in Figure 6a.

Amide I and Amide II. Figure 5 displays second derivatives in the 1700−1500 region of the spectra shown in Figure 4. Of note is that a band appears abruptly at 1653 cm^{-1} near 32.4 °C. The amide II band shifts to a lower frequency by 6 cm^{-1} in the vicinity of 32.4 °C, but its change is more gradual than the changes in the amide I region. The temperature range where the amide I and II bands show distinct changes is in accordance with the reported one as the coil−globule transition temperature.[12,13,16−26] $I(\nu,T)$, $R_{\nu_0}(23.7,T)$, and their first derivatives are represented for the amide I (1653 and 1624 cm^{-1}) and amide II (1562 cm^{-1}) bands in Figure 6 parts a and b, respectively. $I(1653,T)$, $I(1624,T)$, and $I(1562,T)$ show a similar profile with the flexion point near 33.8 °C. All $I(\nu,T)$ shown in Figure 6a start to increase above 31.7 °C. This means that the sedimentation of PNiPA because of the coil−globule transition occurs above 31.7 °C. It

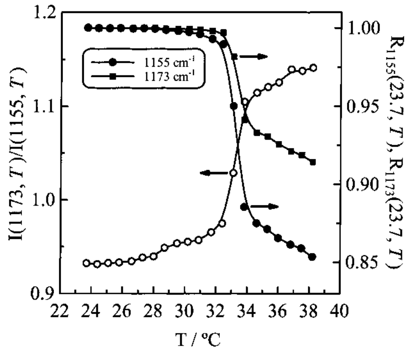

Figure 7. Temperature-dependent change in the intensity ratio of the band near 1173 to 1155 cm^{-1}, $I(1173,T)/I(1155,T)$, and the cross correlation coefficient for these bands, $R_{1173}(23.7,T)$ and $R_{1155}(23.7,T)$.

is noted that $R_{\nu_0}(23.7,T)$ shows different variations; $R_{1653}(23.7,T)$ and $R_{1624}(23.7,T)$ decrease suddenly above 32.4 °C, whereas $R_{1562}(23.7,T)$ decreases gradually from 28.7 °C. The amide II band changes its shape gradually before the transition, and the slope of the change in the shape of the amide II band in the vicinity of the transition temperature is also gradual compared with those of the amide I bands. The reason for this is discussed later. The results indicate that the intensity variations and the changes in the band shapes in the IR spectra of PNiPA do not always synchronize.

Amide III. As shown in Figure 4, the relative intensity of the band at 1173 cm^{-1} is weaker than that of 1155 cm^{-1} below 32.4 °C, but it becomes stronger above 32.4 °C. Referring to the DFT calculation described later, these bands are assigned to the amide III bands, which contains C−N stretching vibrations and N−H bending vibrations. Figure 7 shows temperature-dependent changes in the intensity ratio of the bands at 1173 and 1155 cm^{-1}, $I(1173,T)/I(1155,T)$, and the cross correlation coefficients for these bands, $R_{1173}(23.7,T)$ and $R_{1155}(23.7,T)$. The temperature profile of $I(1173,T)/I(1155,T)$ shows a clear change at the transition temperature. This result indicates that the absorbance intensities of the bands at 1173 and 1155 cm^{-1} reflect the coil−globule transition. The thermal changes in $R_{1173}(23.7,T)$ and $R_{1155}(23.7,T)$ also suggest that each band shape varies near the transition temperature.

4. DFT Calculation for Dimer Models of PNiPA. As mentioned above, the several bands in the IR spectra of the PNiPA aqueous solution are very sensitive to the transition behavior; that is, the changes in bands may be concerned with conformational changes and/or changes in hydrogen bonds of PNiPA during the coil−globule transition. To investigate the relationship between the spectral and structural changes of PNiPA, a simulation using DFT calculation was performed.

The structures of model compounds for PNiPA were optimized at B3LYP/6-31G(d) level and their IR spectra were simulated using the DFT force fields. Seven optimized conformations of the dimer models for PNiPA are illustrated in Figure 8. The main chains of dimer 1, 2, and 3 models assume to be a trans conformation, whereas those of dimer 4, 5, and 6 models do a gauche conformation. In dimer 2 and 5 models, the neighboring C═O groups are close to each other, whereas in dimer 3 and 6 models the neighboring N−H groups face each other. The tacticity of these dimer models is syndiotactic, except dimer model 7 (isotactic). Dimers 1 and 4 have a hydrogen bond between the neighboring amide groups (C═O···H−N). The single-point energy calculation for the optimized structures show that dimer 1 has the most stable structure. The difference energy between dimer 1 and the other dimers is summarized in Table 2. Comparing the models that have the same conformation in the side chain, the result suggests that the trans conformation in the main chain is more stable than the gauche one. Furthermore, when the main chain has the same conformation (trans or gauche), the conformers forming an intramolecular hydrogen bond are more stable than those without the hydrogen bond.

Figure 9 compares the simulated IR spectra for the seven models. The Lorentz type with the bandwidth, full width at the half-height, of 7 cm^{-1} was assumed in each band for simulated spectra. It is of note that the simulated spectra show a marked dependence on the conformation of model compounds. The amide I band of dimers 1 and 4 splits into two bands. The band with the lower frequency arises from the C═O···H−N hydrogen bond, whereas that with the higher frequency is due to the "free" C═O group. Two corresponding bands are observed in the amide II region. The results in Figure 9 reveal that the amide I and amide II bands show a remarkable shift, when the amide groups form the intramolecular hydrogen bond. In the amide I and II regions, the simulated IR spectra for dimers 1 and 4 are

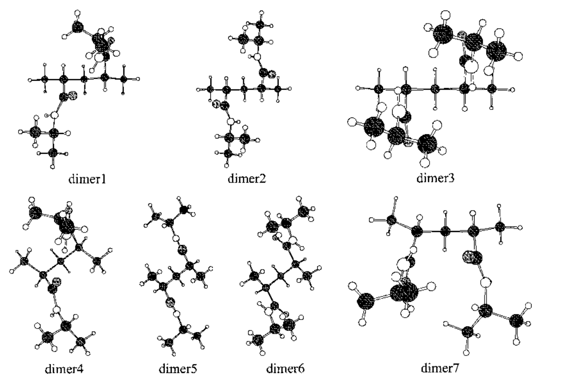

Figure 8. Conformations of dimer models of PNiPA optimized by DFT calculation at the B3LYP/6-31G(d) level.

TABLE 2: Calculated Difference Energies[a] (kcal mol^{-1}) of Dimer Models for PNiPA Using B3LYP Functional of Various Basis Sets and the Onsager Model

basis set	dimer 1	2	3	4	5	6	7
6-31G(d)	0	8.8	2.9	6.9	10.1	8.8	3.2
6-31G(d,p)	0			6.9			
6-31+G(d)	0			7.1			
6-31+G(d,p)	0			7.1			
6-31++G(d,p)	0			7.0			
6-31G(d)[b]	0			6.9			

[a] The energies are represented as the absolute difference energy of the conformer from the energy of dimer 1 calculated at each basis set. [b] The energy was calculated on the basis of the Onsager model.

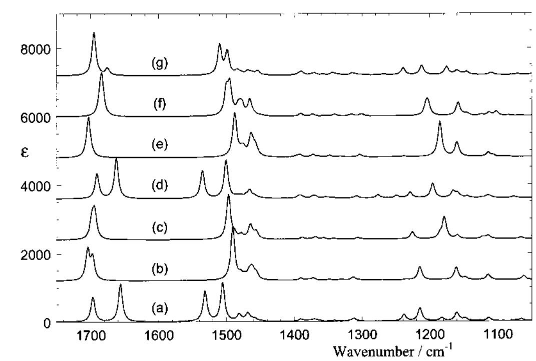

Figure 9. Simulated IR spectra for model compounds displayed in Figure 8; (a) dimer 1, (b) dimer 2, (c) dimer 3, (d) dimer 4, (e) dimer 5, (f) dimer 6, (g) dimer 7.

almost the same. On the other hand, we can find significant differences between them in the amide III region. The C−N stretching mode for dimer 1 is observed at a higher frequency region (about 1215 cm^{-1}) compared with that for dimer 4 (about 1196 cm^{-1}) as shown in Figure 9. This suggests that bands in the amide III region (around 1200 cm^{-1}) are sensitive to the conformational change of model compounds.

As mentioned above, the observed spectra of PNiPA may be interpreted by simulated spectra of dimers 1 and 4. Dimer 1 and 4 models were investigated in more detail by the following calculations: the dependence of simulated spectra on basis sets and the solvation model; the simulated spectra for dimer 1 and 4 models were calculated by using B3LYP functional with the basis sets of 6-31G(d), 6-31G(d,p), 6-31+G(d), 6-31+G(d,p), and 6-31++G(d,p). Although we could not find the basis set that makes the calculated IR spectra perfectly coincident with the observed ones, the differences in the relative intensities in the amide III between the dimer 1 and 4 region are similarly simulated by all of the basis sets used. Of particular note is that irrespective of the basis sets dimer 1 gives the amide III band near 1215 cm^{-1}, whereas dimer 4 yields the corresponding band near 1196 cm^{-1}. Thus, this strongly suggests again that the bands in the 1230−1175 cm^{-1} region are sensitive to conformational changes in the main chain of PNiPA. The difference energies of dimers 1 and 4 using various basis sets are summarized, as seen in Table 2. The results suggest that the difference energy between dimers 1 and 4 does not depend on the choice of the basis sets.

To estimate the effect of hydration on the IR spectra of PNiPA, a well-known and simple hydration model, called the Onsager model,[48−50] was applied. The dielectric constant of water (73.82) and the radius of the sphere cavity (5.4 Å) were assumed. The result indicates that the difference energy between dimers 1 and 4 calculated in the Onsager model is coincident with that without solvation model, as written in Table 2. Hydration of the amide group has more significant influence on the amide I and II bands than on bands because of vibrations of alkyl chains. Upon the hydration, the amide I and II bands arising from the intramolecular hydrogen bond shift distinctly to a lower frequency and a higher frequency, respectively. In contrast, corresponding bands due to the free C═O and N−H groups show only a slight change with the hydration.

Discussion

1. Intramolecular Hydrogen-Bonding of PNiPA. In the observed spectra of PNiPA in an aqueous solution, the amide I and II bands are separated by about 62 cm^{-1}. It can be seen from Figure 9 that only the dimer 1 and 4 model can reproduce this degree of band separation. Other models shows that amide I and amide II bands are separated by more than 180 cm^{-1}. Thus, we can exclude unambiguously other models. It has been well investigated by light scattering studies that the main chain of PNiPA has no stereoregularity.[17,18] Therefore, almost all of the conformations shown in Figure 8 may be allowed as real local conformations for PNiPA. However, a comparison between the experimental results and the simulated IR spectra suggests that only dimers 1 and 4 hold the important structural features as the local conformations.

It is very likely that the band near 1624 cm^{-1} is due to the intramolecular C═O···H−N hydrogen bond and the band at 1653 cm^{-1} arises from the free C═O group. Thus, it seems that almost neighboring amide groups form the intramolecular hydrogen bonds below the θ temperature and that some of the hydrogen bonds are broken during the coil−globule transition. The amide II corresponding to the amide I band at 1653 cm^{-1} band may be observed near 1517 cm^{-1} in Figure 5.

The temperature profile of $R_{1562}(23.7,T)$ is different from those of $R_{1653}(23.7,T)$ and $R_{1624}(23.7,T)$ as shown in Figure 6. That is to say, the thermal changes in the band shape of amide I and II have an asynchronicity. $R_{1562}(23.7,T)$ decreases gradually even below the θ temperature, whereas $R_{1624}(23.7,T)$ shows no variation below the θ temperature. If the band shape in the amide I and II regions was influenced only by the intramolecular hydrogen bonds, both of them would be synchronous. The profile of $R_{1562}(23.7,T)$ seems to be similar to the temperature variation of the gyration radius of PNiPA.[17,18] As is well-known, the gyration radius of PNiPA becomes small gradually below the θ temperature, and then shows an abrupt change in the vicinity of the transition temperature. The thermal response of the amide II band may include the information not only about the changes in the intramolecular hydrogen bond, but also about conformational changes in the main chain. It is likely because the amide II mode contains the contribution from the C−N stretching mode and the simulation study reveals that the C−N stretching mode is influenced by the conformational changes in the main chain of PNiPA. This may be the reason the temperature-dependent change in the amide II band differs slightly from that in the amide I band.

2. Hydration. Many authors reported about the hydration around the polymer segments of PNiPA[20,23−26] because coil−globule transitions of polymers have been explained by changes in the interactions between polymer segments and solvent molecules. That is to say, the dehydration of the polymer chain above the transition temperature induces the segmental interactions of the polymer to be attractive and to collapse the coiled polymer chain into a globular conformation. However, it is not easy to discuss directly the effects of hydration on the IR spectra in the present state. If the low frequency of the amide I band (1624 cm^{-1}) for the aqueous solution were due to the hydration of the amide group, the strong hydration should be considered. The hydration model in the DFT calculation with the Onsager model could not reproduce a large shift of the band arising from the free C═O group. To explore the hydration on the polymer segment by means of the IR spectroscopy, a more realistic model for hydration and more detailed experimental data may be needed.

3. Conformational Changes in the Main Chain of PNiPA. The simulation study reveals that the amide III bands are quite sensitive to the conformational changes in the main chain of PNiPA. One can distinguish between the gauche and trans conformations as the local conformation in the main chain using the amide III bands when the amide groups form the intramolecular hydrogen bond. The structural difference between dimers 1 and 4 lies in the conformation of the main chain: the main chain of the dimer 1 model assumes a trans conformation, whereas that of the dimer 4 model takes a gauche conformation. Although the simulated IR spectra of these dimer models are very similar to each other in the amide I and II regions, distinct spectral changes are observed in the amide III region. As shown in Figure 9, the frequencies of amide III bands vary clearly when the conformation of the main chain alters from gauche to trans. On the other hand, the intensity ratio of the bands at 1173 and 1155 cm^{-1} changes during the transition (Figure 7) without the wavenumber shift of these bands. Comparison between the experimental results and the spectral simulation suggests that the bands at 1173 and 1155 cm^{-1} contain the contribution from the trans and gauche conformations, respectively. Therefore, it is likely that the population of these local conformations varies during the coil−globule transition. That is, the gauche conformation decreases and/or the trans conformation increases when PNiPA change into the globule state.

It is worth noting that above the θ temperature the population of the more stable trans conformation increases and that of the less stable gauche conformation decreases against the Boltzmann's distribution low. Although this is a curious point to discuss, we have no experimental or theoretical explanation in the present state. The following reason may be considered. First, the local conformation is influenced from the stabilization of the whole chain of PNiPA. In other words, the long-range interaction affects the short-range interaction. Second, the stabilization of the local conformation may be susceptible to the solvent around the amide group in terms of not only polarity but also hydration.

Conclusion

The present study has investigated the short-range interaction in the PNiPA aqueous solution mainly due to the hydrogen bonding between neighboring amide groups by use of ATR/IR spectroscopy and DFT calculation. The temperature-dependent IR study of the PNiPA aqueous solution has revealed that the microenvironment around the amide groups is changed dramatically during the coil−globule transition. Below the θ temperature, the unimodal peaks are observed at 1624 (amide I region) and 1562 cm^{-1} (amide II region), respectively. Above the θ temperature, the new peak appears at 1653 cm^{-1} abruptly in the amide I region, and the amide II band shows a gradual upward shift by ca. 6 cm^{-1}. The relative intensity of the band at 1173 cm^{-1} is weaker than that of 1155 cm^{-1} at lower temperatures, and then it becomes stronger during the coil−globule transition of PNiPA. The simulation study by DFT calculation suggests that the neighboring amide groups form an intramolecular hydrogen bond (C═O···H−N), which causes a distinct downward shift of the amide I band and an upward shift of the amide II bands. It has also been implied from the DFT calculation that the conformation changes in the main chain cause variations in the amide III bands (1130−1180 cm^{-1}). Considering both the experimental results and simulations, it has been suggested that some of the intramolecular hydrogen bonds of neighboring amide groups are broken and the populations of the gauche conformation in the polymer chain decreases during the coil−globule transition of PNiPA.

Acknowledgment. The financial support from the Hyogo Science and Technology Association to Y.K. is gratefully acknowledged.

References and Notes

(1) de Genne P. G. *Scaling Concepts in Polymer Physics*; Cornell University Press: Ithaca, NY, 1979.
(2) Doi, M.; Edwards, S. F. *The Theory of Polymer Dynamics*; Clarendon Press: Oxford, U.K., 1986.
(3) Strobl, G. R. *The Physics of Polymers*; Springer-Verlag: Berlin, Germany, 1996.
(4) Ptitsyn, O. B.; Eizner, Y. Y. *Biofizika* **1965**, *10*, 1.
(5) de Genne, P. G. *Phys. Lett. A* **1972**, *38*, 339.
(6) de Genne, P. G. *J. Phys. Lett.* **1975**, *36*, L55.
(7) Nishio, I.; Sun, S. T.; Swislow, G.; Tanaka, T. *Nature* **1979**, *281*, 208.
(8) Sun, S. T.; Nishio, I.; Swislow, G.; Tanaka, T. *J. Chem. Phys.* **1980**, *73*, 5971.
(9) Chu, B.; Park, I. H.; Wang, Q.; Wu, C. *Maclomolecules* **1987**, *20*, 1965.
(10) Nakata, M.; Nakagawa, T. *J. Chem. Phys.* **1999**, *110*, 2703.
(11) Terramoto, T.; Yonezawa, F. *Int. J. Mod. Phys.* B **2000**, *14*, 621
(12) Heskins, M.; Guillet, J. E. *J. Macromol. Sci. Chem.* **1968**, A*2*, 1441.
(13) Hu, H.; Fan, X.-d. *J. Func. Polym.* **2000**, *13*, 461
(14) Hirokawa, Y.; Tanaka, T. *J. Chem. Phys.* **1984**, *81*, 6379.
(15) Dusek, K.; Patterson, D. *J. Polym. Sci.* **1968**, A*2*, 1209.
(16) Fujishige, S.; Kubota, K.; Ando I. *J. Phys. Chem.* **1989**, *93*, 3311.
(17) Kubota, K.; Fujishige, S.; Ando, I. *J. Phys. Chem.* **1990**, *94*, 5154.
(18) Wan, X.; Qiu, X.; Wu, C. *Macromolecules* **1998**, *31*, 2972.
(19) Schild, H. G.; Tirrell. D. A. *J. Phys. Chem.* **1990**, *94*, 4352.
(20) Inomata, H.; Goto, S.; Otake, K.; Saito, S. *Langmuir* **1992**, *8*, 687.
(21) Winnk, F. M. *Macromolecules* **1990**, *23*, 233.
(22) Walter, R.; Rièka, J.; Quellet, C.; Nyffenegger, R.; Binkert, T. *Macromolecules* **1996**, *29*, 4019.
(23) Ohta, H.; Ando, I.; Fujishige, S.; Kubota, K. *J. Polym. Sci., Polym. Phys. Ed.* **1991**, *29*, 963.
(24) Percot, A.; Zhu, X. X.; Lafleur, M. *J. Polym. Sci., Polym. Phys. Ed.* **2000**, *38*, 907.
(25) Maeda, Y.; Higuchi, T.; Ikeda, I. *Langmuir* **2000**, *16*, 7503.
(26) Maeda, Y.; Nakamura, T.; Ikeda, I. *Macromolecules* **2001**, *34*, 1391.
(27) Doty, P.; Wada, A.; Ynag, J. T.; Blout, E. R. *J. Polym. Sci.* **1957**, *23*, 851.
(28) Doty, P. *Rev. Modern Phys.* **1959**, *31*, 107.
(29) Siesler, H. W.; Holland-Moritz, K. *Infrared and Raman Spectroscopy of Polymers*; Mercel Dekker: New York, 1980.
(30) Fujishige, S. *Polymer J.* **1987**, *19*, 297.
(31) Savitzky, A.; Golay, M. J. E. *Anal. Chem.* **1964**, *36*, 1627.
(32) Becke, A. D. *J. Chem. Phys.* **1993**, *98*, 5648.
(33) Johnson, B. G.; Frisch, M. J. *J. Chem. Phys.* **1994**, *100*, 7429.
(34) Ditchfield, R.; Hehre, W. J.; Pople, J. A. *J. Chem. Phys.* **1971**, *54*, 724.
(35) Hehre, W. J.; Ditchfield, R.; Pople, J. A. *J. Chem. Phys.* **1972**, *56*, 2257.
(36) Hariharan, P. C.; Pople, J. A. *Mol. Phys.* **1974**, *27*, 209.
(37) Gordon, M. S. *Chem. Phys. Lett.* **1980**, *76*, 163.
(38) Hariharan, P. C.; Pople, J. A. *Theo. Chim. Acta* **1973**, *28*, 213.
(39) Clark, T.; Chandrasekhar, J.; Spitznagel, G. W.; Schleyer, P. v. R. *J. Comput. Chem.* **1983**, *4*, 294.
(40) Frisch, M. J.; Pople, J. A.; Binkley, J. S. *J. Chem. Phys.* **1984**, *80*, 3265.
(41) Frisch, M. J.; Trucks, G. W.; Schlegel, H. B.; Scuseria, G. E.; Robb, M. A.; Cheeseman, J. R.; Zakrzewski, V. G.; Montgomery, J. A., Jr.; Stratmann, R. E.; Burant, J. C.; Dapprich, S.; Millam, J. M.; Daniels, A. D.; Kudin, K. N.; Strain, M. C.; Farkas, O.; Tomasi, J.; Barone, V.; Cossi, M.; Cammi, R.; Mennucci, B.; Pomelli, C.; Adamo, C.; Clifford, S.; Ochterski, J.; Petersson, G. A.; Ayala, P. Y.; Cui, Q.; Morokuma, K.; Malick, D. K.; Rabuck, A. D.; Raghavachari, K.; Foresman, J. B.; Cioslowski, J.; Ortiz, J. V.; Stefanov, B. B.; Liu, G.; Liashenko, A.; Piskorz, P.; Komaromi, I.; Gomperts, R.; Martin, R. L.; Fox, D. J.; Keith, T.; Al-Laham, M. A.; Peng, C. Y.; Nanayakkara, A.; Gonzalez, C.; Challacombe, M.; Gill, P. M. W.; Johnson, B. G.; Chen, W.; Wong, M. W.; Andres, J. L.; Head-Gordon, M.; Replogle, E. S.; Pople, J. A. *Gaussian 98*, revision A.9; Gaussian, Inc.: Pittsburgh, PA, 1998.
(42) Bauschlichter, C. W., Jr.; Partridge, H. *J. Chem. Phys.* **1995**, *103*, 1788.
(43) Onsager, L. *J. Am. Chem. Soc.* **1938**, *58*, 1486.
(44) Wiberg, K. B.; Murcko, M. A. *J. Phys. Chem.* **1987**, *91*, 3616.
(45) Mirabella, F. M., Jr., Ed.; *Internal Reflection Spectroscopy; Theory and Application*; Marcel Dekker: New York, 1993.
(46) Powell, J. R.; Wasacz, F. M.; Jakobsen, R. J. *Appl. Spectrosc.* **1986**, *40*, 339.
(47) Dousseau, F.; Therrien, M.; Pézolet, M. *Appl. Spectrosc.* **1989**, *43*, 538.
(48) Wong, M. W.; Frisch, M. J.; Wiberg, K. B. *J. Am. Chem. Soc.* **1991**, *113*, 4776.
(49) Wong, M. W.; Wiberg, K. B.; Frisch, M. J. *J. Am. Chem. Soc.* **1992**, *114*, 523.
(50) Wong, M. W.; Wiberg, K. B.; Frisch, M. J. *J. Chem. Phys.* **1991**, *95*, 8991.